A New Research on Contrast Sensitivity Function Based on Three-Dimensional Space

Jiachen Yang[1], Yun Liu[1,2](✉), Wei Wei[3], Qinggang Meng[4], Zhiqun Gao[1], and Yancong Lin[1]

[1] School of Electronic Information Engineering, Tianjin University, Tianjin 300072, China
{yangjiachen,yunliu}@tju.edu.cn, {gaozhiqunzz,linyc551}@163.com
[2] School of Optometry, University of California, Berkeley, Berkeley, CA, USA
yunliusally@berkeley.edu
[3] School of Computer Science and Engineering, Xi'an University of Technology, Xi'an 710048, Shanxi, China
weiwei@xaut.edu.cn
[4] Department of Computer Science, School of Science at Loughborough University, Loughborough LE11 3TU, UK
q.meng@lboro.ac.uk

Abstract. In this paper, we try to extend human eyes' contrast sensitivities characteristics (CSF) to three-dimensional space, but the experimental results show that the traditional characteristics of CSF has limitations in three-dimensional space. In order to investigate the characteristics of human eyes' CSF in three-dimensional space, the traditional CSF test method is developed to measure the corresponding values of CSF in different inclined planes in three-dimensional space. Human visual contrast sensitivity characteristics with different inclined angles θ are analyzed, and the mathematical expression of $\theta - CSF$ is built up based on the experimental results. The proposed $\theta - CSF$ model of three-dimensional space in this paper can well reflects human visual contrast sensitivity characteristics in 3D space and has significant effect on three-dimensional image processing.

Keywords: Human visual system · Contrast sensitivity function · Spatial frequency · Three-dimensional space

1 Introduction

With the development of science and technology, information processing technology is becoming more mature [1]-[4]. In order to really reflect what people seen in the natural scene, human visual system (HVS) is often incorporated into the technology of image processing [5],[6]. The most important one among human visual characteristics in HVS is the contrast sensitivity characteristic [7],[8] which has been widely used in the area of image processing in plane space [9],[10]. Chen *et al.* [11] proposed a perceptual quality evaluation method for

H. Zha et al. (Eds.): CCCV 2015, Part II, CCIS 547, pp. 417–428, 2015.
DOI: 10.1007/978-3-662-48570-5_40

image fusion based on CSF which is focus on the night vision application; Tao *et al.* [12] developed a novel reduced-reference image quality assessment scheme by incorporating CSF and the objective assessment results, which can well reflect the visual quality of images. Some effective quality assessment methods also effectively built by incorporating CSF characteristics and wavelet transforms of image, such as Gao [13] and Li [14], which can well reflect human visual perception. Besides, Zhang [15], Wu [16] and Müller [17] *et al.* applied CSF characteristic to the technology of image processing and made great achievements. Urvoy [18] and Tsai [19] *et al.* proposed an effective perceptual watermarking technique based on CSF and achieved good robustness against the common operations.

The characteristic of human eyes' traditional CSF (in this paper CSF proposed by the predecessors called traditional CSF) is built based on the grating test system, in which the monitor paralleled to the viewer's face in two-dimensional (2D) space without considering other inclined planes that not paralleled to human face. The traditional CSF is just aim at the plane display technologies, such as 2DTV and 2D movie. In fact, what people see in the real world are not all displayed on the plane paralleled to human face. With the development of three-dimensional image processing technology and display technology [20],[21], more and more 3D displays are widely used, such as 3DTV, holographic display and so on. Whether traditional CSF suits for three-dimensional space has not been verified, and limited its application in three-dimensional space. It is very necessary to study human visual contrast sensitivity characteristics in 3D space.

The rest of this paper is organized as follows. In Section 2, it describes the theory of the traditional CSF. Section 3 the extension of traditional CSF in three-dimensional space is illustrated. And the comparison between experiment results and the results of the extension of traditional CSF is showed in Section 4. In Section 5, the model of CSF in three-dimensional space is built. Finally, conclusion and future work are given in Section 6.

2 An Overview of Traditional CSF

Human eyes have different visual characteristics in different frequency bands, i.e., we are unable to recognize a stimuli pattern if its frequency of visual stimuli is too high. For example, given an image consisting of horizontal black and white stripes, we will perceive it as a gray image if stripes are very thin; otherwise, we can distinguish these stripes. Based on the visual characteristics, traditional contrast sensitivity function (CSF) has been proposed which measures how sensitive we are to the various spatial frequencies of visual stimuli. Now the value of traditional CSF can be measured by grating contrast sensitivity test system (shows in Fig.1.(a)) which has been used to study the physiology of the visual system [22] for some time and increasingly used to study ophthalmology [23]. Unlike the Snellen letter acuity test [24], which establishes visual acuity in terms of the smallest recognizable object presented at 100% contrast, the grating test allows the specification of an observer's sensitivity to larger targets of lower contrast, and sensitivity is defined as the reciprocal of the contrast threshold. Mannos and

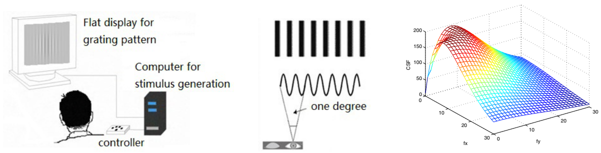

(a) (b) (c)

Fig. 1. (a)Traditional CSF test system: the observers view the gratings monocular with the fellow eye occluded (b) The concept of spatial frequency:two circles per degree. (c)2D CSF characteristics surface

Sakrison [25], after conducting a series of psychophysical experiments on human subjects, found that CSF can be modeled by the function in Eq.(1).

$$A(f) = (0.0499 + 0.2964f)e^{-(0.114f)^{1.1}} \tag{1}$$

where f is the spatial frequency which means the number of cycles per degree subtended at the eye (shows in Fig.1.(b)), with unit of cycles/degree. Eq.(1) reveals that the values of traditional CSF are related with the circles of grating in human eyes (that is f).

Generally in image processing area, human visual system has the same contrast sensitivity in all directions of plane space, and the 2D version [26] can be easily obtained by replacing f with radial frequency $\sqrt{f_x^2 + f_y^2}$

$$A = (0.0499 + 0.2964\sqrt{f_x^2 + f_y^2})e^{-(0.114\sqrt{f_x^2+f_y^2})^{1.1}} \tag{2}$$

where f_x and f_y are the horizontal and vertical frequencies respectively, and they make no sense for frequencies above 30 cycles/degree. Fig. 1(c) shows the 2D CSF characteristics surface.

3 The Extension of Traditional CSF in Three-Dimensional Space

Traditional CSF is a nonlinear function of spatial frequency which is built based on the plane of two-dimensional space (such as plane 1 shows in Fig.2(a)). Here we try to extend it to three-dimensional space including many inclined planes such as plane 2 and plane 3. Because of the existence of inclined angles (θ_1 and θ_2 show in Fig.2(a)), the value of spatial frequency in the inclined plane will be changed. Based on the theory of traditional CSF, the values of CSF in different inclined planes can be get by applying the spatial frequency of each inclined plane to Eq.(1). To verify the practicability of traditional CSF in 3D space, subjective experiments, shown in Fig.2(b) (to get the inclined plane by rotating the test monitor), are conducted to study the relationship between calculated

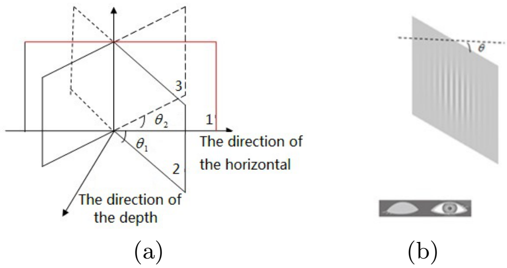

Fig. 2. (a) Geometric simulation figure of three-dimensional image (b) CSF test system of different inclined plane.

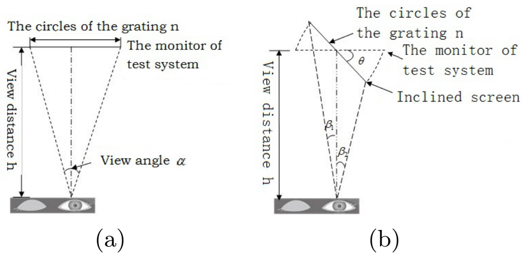

Fig. 3. (a) Geometric simulation figure of test system of traditional CSF (b) Geometric simulation figure of test system of CSF in the inclined plane

CSF values based on Eq.(1) and the experimental data on different inclined planes, and investigate human eyes' characteristics of CSF in three-dimensional space.

According to the test theory of traditional CSF, the monitor of test system is set to paralleled to viewers' face, the observers viewed the gratings monocular with the fellow eye occluded and the view angle is α (shows in Fig.3(a)). Define the circles of grating in human eyes as n, and the viewing distance is h (the value is far greater than n). After rotating the monitor clockwise to form the inclined angle θ (shows in Fig.3(b)), the circles of grating is still n, because what the observer see is the same monitor and the circles of gratings are not change, while the view angle is changed to $\beta_1 + \beta_2$, so the spatial frequency f is changed. Based on the concept of the spatial frequency [27] shown in Eq.(3).

$$f(\frac{cycles}{degree}) = \frac{f_i}{\arcsin \frac{1}{\sqrt{[1+d^2(H^2+V^2)]}}} \tag{3}$$

where f_i is the image frequency (obtained from Fourier transform), the normalizing factor f_n is the number of pixels within 1 degree at the viewing distance of d times the diagonal image size, H is the horizontal image size and V is the vertical image size in pixels. Based on the geometrical relationships, we have:

$$f_u(\frac{cycles}{degree}) = \frac{n}{\alpha} \tag{4}$$

$$f_\theta(\frac{cycles}{degree}) = \frac{n}{\beta} \tag{5}$$

where $\beta = \beta_1 + \beta_2$. f_u, horizontal spatial frequency, is the spatial frequency of the plane with inclined angle 0°; f_θ, inclined spatial frequency, is the spatial frequency of the inclined plane with inclined angle θ; Because h is far greater than n, so the viewing angle is very small. According to the mathematical theory, when an angle is too small, the value of tangent of the angle and the value of angle are approximately equal. So:

$$\alpha = 2arctan\frac{n/2}{h} \approx 2 \times \frac{n/2}{h} = \frac{n}{h} \tag{6}$$

$$\begin{aligned}\beta &= arctan\frac{\frac{n}{2}cos\theta}{h + \frac{n}{2}sin\theta} + arctan\frac{\frac{n}{2}cos\theta}{h - \frac{n}{2}sin\theta} \\ &\approx \frac{\frac{n}{2}cos\theta}{h + \frac{n}{2}sin\theta} + \frac{\frac{n}{2}cos\theta}{h - \frac{n}{2}sin\theta}\end{aligned} \tag{7}$$

From the above analysis, the horizontal spatial frequency f_u and the inclined spatial frequency f_θ are obtained:

$$f_u = \frac{n}{\alpha} \approx h \tag{8}$$

$$f_\theta = \frac{n}{\beta} \approx \frac{n}{hncos\theta/(h^2 - \frac{n^2}{4}sin^2\theta)} \tag{9}$$

Because h is far greater than n, so :

$$h^2 - \frac{n^2 sin^2\theta}{4} \approx h^2 \tag{10}$$

$$f_\theta = \frac{n}{\beta} \approx \frac{h}{cos\theta} \tag{11}$$

Then the relationship between the horizontal spatial frequency f_u and the inclined spatial frequency f_θ is given by :

$$f_\theta = f_u/cos\theta \tag{12}$$

Besides, based on the geometric symmetry, it can be easily get the conclusion: when the monitor of the test system rotated counterclockwise (plane 3 in Fig.2(a)), the corresponding spatial frequency in these inclined directions and the horizontal spatial frequency are all meet the mathematical expression of Eq.(12). And together with the expression of traditional CSF and the replacement of f in Eq.(1) by $f_u/cos\theta$, the CSF's expressions of each inclined plane is expressed by:

$$A(f_\theta) = (0.0499 + 0.2964(f_u/cos\theta))e^{-(0.114(f_u/cos\theta))^{1.1}} \quad (13)$$

To verify the correctness of Eq.(13), the rest work in the paper will take the clockwise rotation direction as an example, and use the grating test system to test the values of contrast sensitivities in different inclined planes when observers view the monitor monocular with the fellow eye occluded.

4 The Comparison between Experiment Result and the Result of Extension of Traditional CSF

This work firstly tests the value of human eyes' traditional CSF values to verify the reliability of the experimental data and then rotated the monitor of the test system to form different inclined angles. The values of CSF in different inclined planes is measured and verified whether the above $A(f_\theta)$ meet human visual characteristics.

The gratings of the test system are electronically generated on the screen of a monochrome television monitor (Melford Electronics DU1/20, 625 lines, 50Hz, 2:1 interlaced, P4 phosphor). The experiments are performed under photopic conditions with the mean luminance of the gratings constant at $100cd/m^2$. The television screen is subtended $180 \times 15°$. To minimize fading at low spatial frequencies and the generation of after-images the gratings are continuously reversed at the rate of $1cycles/s$ and observers are instructed to fixate a small spot in the center of the screen. The observers view the gratings monocular with the fellow eye occluded. At each spatial frequency the contrast of the grating is reduced by means of a potentiometer until the observer indicate that the grating is just disappeared, then record the contrast value as the threshold of this spatial frequency.

We select 18 observers, age from 20 to 40 years, to conduct this experiment. Before the test, all subjects receive a complete clinical evaluation to ensure that their visual fields, color vision, and intraocular pressure within the normal range for the Clinical Branch of the National Eye Institute. All subjects receive a fundus evaluation by a staff ophthalmologist to ensure that there is no detectable ocular pathology affecting either retinal or preretinal (e.g., cataract) levels within the eye. In addition, each subject receive a complete refractive evaluation before testing. All subjects have best-corrected visual acuities of 20/20 or better in both eyes. Before the grating tests officially start, the observers take a period of time to adopt to the experiment process. Every observer conducts this experiments

Table 1. CSF test values of observers

f_u	2	4	8	16	32
CSF_0	0.3786	0.7849	0.9862	0.7270	0.1233
$CSF_{\frac{\pi}{4}}$	0.3434	0.7849	0.9862	0.4227	0.0971
$CSF_{\frac{\pi}{3}}$	0.3663	0.7849	0.9862	0.4371	0.1028

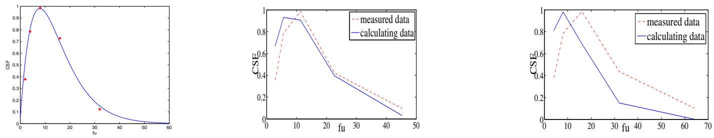

(a) (b) (c)

Fig. 4. (a) Comparison results between test result with the inclined angle 0° and traditional CSF curve. (b)The fitting curve with the inclined angle of $\frac{\pi}{4}$ (c)The fitting curve with the inclined angle of $\frac{\pi}{3}$

twice and the mean value is calculated as the final data. Then human eyes' contrast sensitivities test value is defined as the mean of 18 observers' independent decisions. The values of observers' CSF in the plane with inclined angle 0° is tested at the beginning of the project and the range of the spatial frequency of the test system is from $2circles/degree$ to $32circles/degree$. The result is shown in Table 1, the first row.

The test data is normalized within 1 and frequencies above $60cycles/degree$ is meaningless in reality. Compared with the traditional CSF curve, the test results, as shown in Fig.4(a), are accurate. Then two inclined angles, $\frac{\pi}{4}$ and $\frac{\pi}{3}$ are set to carry out the experiment, the test data shown in Table 1, the second and third rows. With the function of $A(f_\theta)$, the CSF values of the inclined planes with the inclined angles $\frac{\pi}{4}$ and $\frac{\pi}{3}$ are calculated. The test results and the calculated values are shown in Fig.4(b) and (c). Fig.4(b) and (c) indicate a great difference between experiment results and calculated values, which means that traditional CSF has limitations in three-dimensional space, and cannot be expanded to three-dimensional space directly.

5 The Proposal of CSF in Three-Dimensional Space

In order to build human eyes' CSF in different inclined planes, it is necessary to obtain data from more inclined angles and values of observers' contrast sensitivities, so $\frac{\pi}{12}$,$\frac{\pi}{6}$ and $\frac{5\pi}{12}$ are set to test. The results shown in Table 2, and fitted shown in Fig.5 (a) and (b) with the amplitude normalized within [0,200]. Using geometry relationship to analyze the test data, it reveals that the curve trends of different inclined angles are the same and all of them have the nature of band pass filter.

Table 2. Human eyes' test values of CSF with different inclined angles

f_u	2	4	8	16	32
$CSF_{\frac{\pi}{12}}$	0.4227	0.9185	0.9862	0.7849	0.1378
$CSF_{\frac{\pi}{6}}$	0.4634	0.9158	0.9862	0.7849	0.1233
$CSF_{\frac{5\pi}{12}}$	0.3434	0.9158	0.7849	0.3260	0.0986

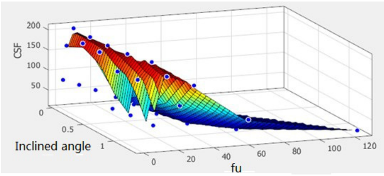

(a)

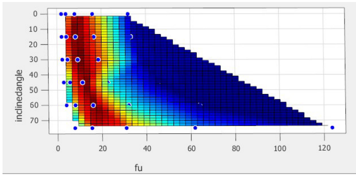

(b)

Fig. 5. (a)The fitting surface of the experiment data. (b) The vertical view of fitting surface.

Specifically, contrast sensitivities of human eyes are different in varied inclined planes; all CSF characteristic curves experience the same trend at different stereo-angles and all have the nature of band pass filter, but the position of the peaks are gradually moved back with the increased inclined angle; besides, the descending velocity of the curve at the high spatial frequency gradually decreased with the increased inclined angle; what's more, the CSF curves in each inclined plane are all like the traditional CSF curve, so it is possible for us to build the θ-CSF's expression of each inclined plane $A(f_\theta, \theta)$ based on the traditional CSF's expression, as follows:

$$A(f_\theta, \theta) = (a + bf_\theta)e^{-(cf_\theta)^d} \tag{14}$$

where f_θ is spatial frequency of the inclined plane with inclined angle θ.

Based on the experimental results, we apply MATLAB fitting tool to obtain the specific value of each parameter, shown in Table 3. Each equation is well fitted with fitting coefficient $R-square > 0.9$, while the values of RMSE are less than 0.4. Table 3 indicates that among all parameters only b and c are changed, and other coefficients are the same as those in traditional CSF under different inclined angle θ. In order to get a general $\theta-CSF$ model, the relationship between b and θ, and c and θ are fitted, shown in Fig.6, which indicate a cosine relationship between b (c) and the inclined angle θ. The good linear correlation with the Pearson correlation coefficients $r > 0.9$ indicates the goodness of the fit. Then the expression of $\theta - CSF$ based on the inclined angles θ in three-dimensional space is defined as Eq.(15):

$$A(f, \theta) = (0.0499 + 0.2964f \times cos\theta)e^{-(0.114f \times cos\theta)^{1.1}} \tag{15}$$

Here the inclined angles are in the unit of radians.

Table 3. Parameters of each inclined plane

$A(f_\theta, \theta)$	a	b	c	d
$A(f_0, 0)$	0.0499	0.2964	0.114	1.1
$A(f_{\frac{\pi}{12}}, \frac{\pi}{12})$	0.0499	0.2863	0.1101	1.1
$A(f_{\frac{\pi}{6}}, \frac{\pi}{6})$	0.0499	0.2567	0.0987	1.1
$A(f_{\frac{\pi}{4}}, \frac{\pi}{4})$	0.0499	0.2096	0.0806	1.1
$A(f_{\frac{\pi}{3}}, \frac{\pi}{3})$	0.0499	0.1482	0.0570	1.1
$A(f_{\frac{5\pi}{12}}, \frac{5\pi}{12})$	0.0499	0.0767	0.0295	1.1

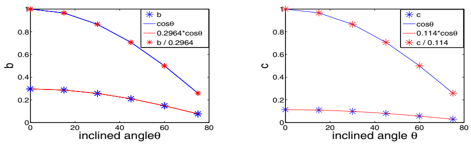

(a) (b)

Fig. 6. (a)The fitted model of b. (b) The fitted model of c.

We quantifies the goodness of the fits with a Q measure given in the figures. Q is a χ^2 distribution function, and Q of 0.1 suggests an acceptable model fit [28]. Each sub-figure provides a very good fit for $Q > 0.1$, which indicates that this model is able to fit our psychophysical data. The surface of the $\theta - CSF$ is illustrated in Fig.8(a), it reveals that the data are agree with the above test values in Fig.5(a). Besides, the CSF curve with the inclined angle 0° are the same as the traditional CSF curve and the vertical view shown in Fig.8(b) coincide with that in Fig.5(b). These results indicate that the proposed $\theta - CSF$ here is in according with human visual characteristics.

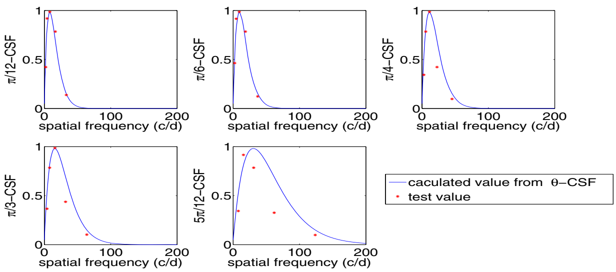

Fig. 7. Comparision results between test value and caculated value from proposed $\theta - CSF$

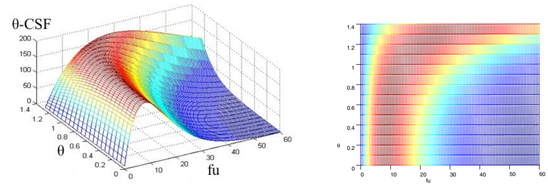

(a) (b)

Fig. 8. (a)$\theta - CSF$ characteristics surface in three-dimensional space. (b) The vertical view of $\theta - CSF$ characteristics surface.

6 Conclusion

This paper aims to apply the concept of the plane spatial frequency to analyze the relationship among different inclined plane, and to extend the traditional CSF to three-dimensional space. According to the experimental results and the geometric relationship between horizontal spatial frequency and the spatial frequency in the directions of inclined angles, $\theta - CSF$ characteristic surface of human eyes based on the inclined angle is built with a specific function expression. The proposed CSF characteristics in three-dimensional space is consistence with human visual characteristics.

Acknowledgments. This research is supported by the National Natural Science Foundation of China (No.61471260 and No.61271324), and Program for New Century Excellent Talents in University (NCET-12-0400).

References

1. Legg, P.A., Rosin, P.L., Marshall, D., Morgan, J.E.: Feature Neighbourhood Mutual Information for Multi-Modal Image Registration: An Application to Eye Fundus Imaging. Pattern Recognition **48**(6), 1937–1946 (2015)
2. Martinez, F., Carrasco, A., Salas, J., di Baja, G.S.: Pattern Recognition Application in Computer Vision and Image Analysis. Pattern Recognition **48**(4), 1025–1026 (2015)
3. Smith, S., Williams, I.: A Statistical Method for Improved 3D Surface Detection. IEEE Signal Processing Letters **22**(8), 1045–1049 (2015)
4. Wei, W., Qi, Y.: Information Potential Fields Navigation in Wireless Ad-Hoc Sensor Networks. Sensors **11**(5), 4794–4807 (2011)
5. Peng, R.B., Varshney, P.K.: A Human Visual System-Driven Image Segmentation Algorithm. Journal of Visual Communication and Image Representation **26**, 66–79 (2015)
6. Chang, H.W., Zhang, Q.W., Wu, Q.G., Gan, Y.: Perceptual Image Quality Assessment by Independent feature detector. Neurocomputing **151**(10), 1142–1152 (2015)

7. Rosén, R., Lundström, L., Venkataraman, A.P., et al.: Quick Contrast Sensitivity Measurements in the Periphery. Journal of Vision **14**(8) (2014)
8. Liu, R., Zhou, J.W., et al.: Immature Visual Neural System in Children Reflected by Contrast Sensitivity with Adaptive Optics Correction. Scientific Reports **4**(4687), April 2014
9. Wei, Z.Y., Ngan, K.N.: Spatio-Temporal Just Noticeable Distortion Profile for Grey Scale Image/Video in DCT Domain. IEEE Transactions on Circuits and Systems for Video Technology **19**(3), 337–346 (2009)
10. Brandᾶ, T., Queluz, M.P.: No-Reference Quality Assessment of H.264/AVC Encoded Video. IEEE Transactions on Circuits and Systems for Video Technology **20**(11), 1437–1447 (2010)
11. Chen, Y., Blum, R.S.: A New Automated Quality Assessment Algorithm for Image Fusion. Image and Vision Computing **27**(2), September 2009
12. Tao, D., Li, X., Lu, W., Gao, X.: Reduced-Reference IQA in Contourlet Domain. IEEE Transaction on Systems Man and Cybernetics-Part B: Cybernatics **39**(6), December 2009
13. Gao, X., Lu, W., Tao, D., Li, X.: Image Quality Assessment Based on Multiscale Geometric Analysis. IEEE Transactions on Image Processing **18**(7), July 2009
14. Li, S., Zhang, F., Ma, L., Ngan, K.N.: Image Quality Assessment by Separately Evaluating Detail Losses and Additive Impairments. IEEE Transactions on Multimedia **13**(5), October 2011
15. Zhang, F., Ma, L., Li, S., Ngan, K.N.: Practical Image Quality Metric Applied to Image Coding. IEEE Transactions on Multimedia **13**(4), August 2011
16. Wu, G.-L., Wu, T.-H., Chien, S.-Y.: Algorithm and Architecture Design of Perception Engine for Video Coding Applications. IEEE Transactions on Multimedia **13**(6), December 2011
17. Müller, K., Merkle, P., Wiegand, T.: 3-D Video Representation Using Depth Maps. Proceedings of the IEEE **99**(4), 643–656 (2011)
18. Urvoy, M., Goudia, D., Autrusseau, F.: Perceptual DFT Watermarking With Improved Detection and Robustness to Geometrical Distortions. IEEE Transactions on Information Forensics and Security **9**(7), 1108–1119 (2014)
19. Tsai, M.J., Liu, J., Yin, J.S., Yuadi, I.: A Visible Wavelet Watermarking Technique based on Exploiting the Contrast Sensitivity Function and Noise Reduction of Human Vision System. Multimedia Tools and Applicatios **72**(2), 1311–1340 (2014)
20. Boisvert, J., Drouin, M.A., Jodoin, P.M.: High-Speed Transition Patterns for Video Projection, 3D Reconstruction, and Copyright Protection. Pattern Recognition **48**(3), 720–731 (2015)
21. Elaiwat, S., Bennamoun, M., Boussaid, F., et al.: A Curve Let-based Approach for Textured 3D Face Recognition. Pattern Recognition **48**(4), 1235–1246 (2015)
22. Schade, S.R.: Optical and Photoelectric Analog of the Eye. Journal of the Optical Society of America **46**(9), 721–738 (1956)
23. Bodis-Wollner, I., Diamond, S.P.: The Measurement of Spatial Contrast Sensitivity in cases of Blurred Vision Associated with Cerebral Lesions. Journal of Neurology **99**, 695–710 (1976)
24. Mocan, M.C., Najera-Covarrubias, M., Wright, K.W.: Comparison of Visual Acuity Levels in Pediatric Patients with Amblyopia using Wright Figures((c)), Allen Optotypes, and Snellen Letters. Journal of Aapos **9**, 48–52 (2005)
25. Mannos, J.L., Sakrison, D.J.: The Effects of a Visual Fidelity Criterion on the Encoding of Images. IEEE Transactions on Information Theory **IT-20**(4), July 1974

26. Zeng, W., Daly, S., Lei, S.: An Overview of the Visual Optimization Tools in JPEG 2000. Signal Processing: Image Communication **17**(1), 85–104 (2002)
27. Gaddipatti, A., Machiraju, R., Yagel, R.: Steering Image Generation with Wavelet Based Perceptual Metric. Computer Graphics Forum **16**(3), C241–C251 (1997)
28. Press, W.H., Teukolsky, S.A., Vetterling, W.T., Flannery, B.P.: Numerical Recipes in C: The Art of Scientific Computing. Cambridge Univ. Press (1992)